Sensors & Actuators: B. Chemical 390 (2023) 134033

Contents lists available at ScienceDirect

Sensors and Actuators: B. Chemical

journal homepage: www.elsevier.com/locate/snb

A cost-effective microfluidic device for determination of biodiesel content in diesel blends

Samara Soares [a,b,1], Celia E. Ramos-Lorente [a,1], Isidoro Ruiz-García [c,d], Fábio R.P. Rocha [b,*], Miguel M. Erenas [a,d,**], Ignacio de Orbe-Payá [a,d], Nuria López-Ruiz [c,d], Luis F. Capitán-Vallvey [a,d]

[a] ECsens, Department of Analytical Chemistry, University of Granada, Granada, Spain
[b] Center for Nuclear Energy in Agriculture, University of São Paulo, Av. Centenário, 303, 13416-000 Piracicaba, SP, Brazil
[c] ECsens, CITIC-UGR, Department of Electronics and Computer Technology, University of Granada, Granada, Spain
[d] Unit of Excellence in Chemistry Applied to Biomedicine and the Environment, University of Granada, Granada, Spain

ARTICLE INFO

Keywords:
Microfluidics
Digital image colorimetry
Quality control
Alkyl esters content
Renewable fuel
Diesel blends

ABSTRACT

The increasing production and extensive use of biodiesel in the latest years call for the development of fast and cost-effective procedures for point-of-care analysis. One of the main quality parameters is the biodiesel content in diesel blends, which needs to conform to regional legislations. In this work, a microfluidic device exploiting chemical derivatization of alkyl esters and detection by smartphone-based digital-image colorimetry was developed. It was designed to ensure proper experimental conditions for chemical derivatization, including reagent release, and photometric measurements. Analytes reacted with alkaline hydroxylamine yielding the corresponding alkyl hydroxamates, measured as colored Fe(III) complexes. Analytical response was based on the measurement of the G (green) channel from RGB color system. By taking methyl linoleate as a model compound, a linear response was obtained from 0.1% to 0.6%(v/v) (Analytical signal = 69.6 +2.1 C, r = 0.999), coefficient of variation (n = 10) of 4.0% and limit of detection (99.7% confidence) of 0.04%(v/v). Procedure consumes 1.2 μL of sample, 230 μg of hydroxylamine, 480 μg of NaOH, 14 μg of Fe(III) and equivalent to 1.2 μL of 69%(v/v) HNO_3. Accurate results were achieved in relation to the MIR reference method, with agreement at the 95% confidence level.

1. Introduction

Biodiesel is an alternative fuel with a great economic and environmental relevance. It is produced from renewable sources, such as vegetable oils and animal fats, and significantly reduces the emission of greenhouse gases (e.g. carbon dioxide) compared to fossil fuels [1,2]. Biodiesel is commercially available as diesel blends, and its amount in the mixture varies according to the legislation of each country. For example, in Brazil, biodiesel was introduced in the energetic matrix in 2005 and the amount gradually increased from 2% (v/v) to 10% (v/v) in 2022 [3]. Germany, France, and Spain are the EU's largest producers of biodiesel [4]. Despite its wide applicability, biodiesel production costs are higher than diesel, making it essential to monitor its amount in diesel blends to ensure legislation compliance and to prevent from fraud [2,5].

The official analytical method to quantify biodiesel in diesel blends is based on mid-infrared spectroscopy (MIR) [5]. Although portable MIR spectrometer is available to perform point-of-care analysis (POC), data processing is time-consuming and requires expertise in chemometrics and a representative number of reference standards to obtain a robust model. Alternative procedures typically involve several analytical steps and require significant amounts of toxic solvents, such as 10 mL of heptane [6] or 5 mL of hexane [7], thus generating substantial waste amounts, e.g. 102 mL [7] or 17 mL [6] per determination. To circumvent these drawbacks and aiming at a more environmentally friendly approach, a flow-based method [8] and a spot test combined with digital-image photometry [9] were proposed. However, despite some analytical advantages, these approaches are limited for POC (e.g. directly at fuel stations), either because of the lack of portability [8] or

* Corresponding author.
** Corresponding author at: ECsens, Department of Analytical Chemistry, University of Granada, Granada, Spain.
E-mail addresses: frprocha@cena.usp.br (F.R.P. Rocha), erenas@ugr.es (M.M. Erenas).
[1] These author contributed equally to this work.

https://doi.org/10.1016/j.snb.2023.134033
Received 4 April 2023; Received in revised form 25 May 2023; Accepted 26 May 2023
Available online 27 May 2023

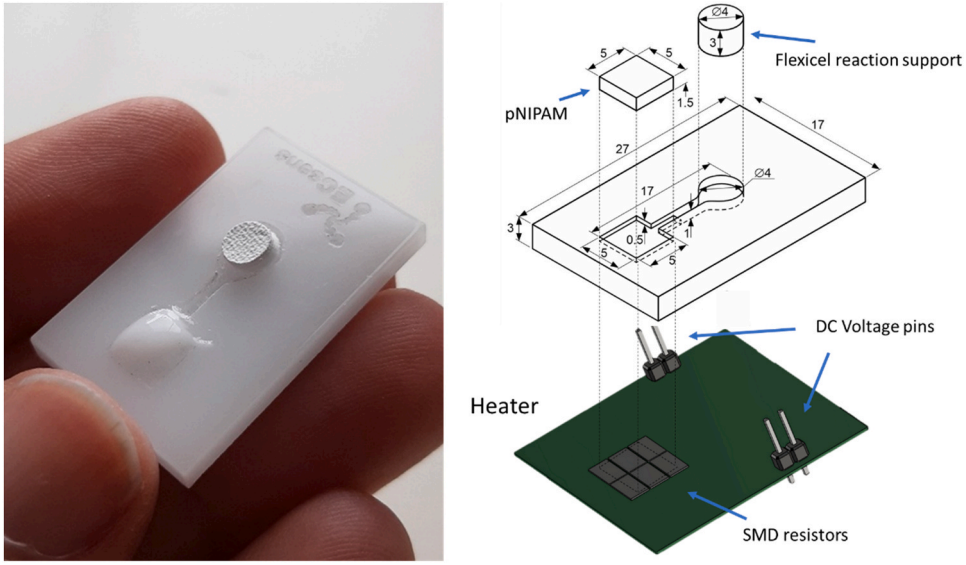

Fig. 1. Photography (left) and schematic representation (right) of the microfluidic device. Distances are given in mm.

the several steps involved in sample processing [9].

Microfluidic devices have been successfully applied for POC, with few, if any, sample pretreatment, making feasible obtaining the analytical results in a fast manner, with minimized consumption of both reagents and solvents [10]. These devices can be designed using different materials, such as silica, glass or polymers. The pioneering article using paper as support, published in 2007, changed the paradigm of microfluidic devices by exploiting a cheaper, widely available, and biodegradable material [11]. In 2011, thread or cloth, including cotton, nylon and other fibers started to be used as reagent support [12–16]. Recent approaches have also exploited magnetic materials [17]. Microfluidics has also been successfully coupled with detection by smartphone-based digital-image colorimetry leading to a wide variety of applications [12], such as the determination of glucose in blood [18] or Cu(II) in sugar cane spirits [19]. Despite the inherent advantages and the high potential to be applied in analysis of biodiesel and biodiesel/diesel blends, microfluidic devices were not exploited to this purpose yet.

Aiming at analytical applications, digital images are usually captured under constant and controlled lighting, usually provided by a white light source, distance from the object to the camera, and region of interest (ROI) [20]. Subsequently, the images are converted to a suitable color system, for example, RGB (*Red, Green, Blue*), CMY (*Cyano, Magenta, Yellow*) and HSV (*Hue, Saturation, Value)*, using specific applications, such as Colorgrab® [21] and Photometrix® [22], or softwares, e.g. ImageJ® [23]. The RGB color system, which predominates in analytical applications, mimics human vision, exploiting the red, green and blue components to reproduce the visible electromagnetic spectrum as ca. 16.7 million colors (256^3). In a vector representation, (0,0,0) represents the total absorption of the incident radiation, whereas (255,255,255) refers to the total reflection of the incident radiation [24].

In this context, the goal of this work is to develop a simple, eco-friendly, portable, and cost-effective microanalytical procedure for the determination of biodiesel in diesel blends exploiting chemical derivatization with hydroxylamine/Fe(III). Reagent immobilization on poly (N-isopropylacrylamide) polymer (pNIPAM) was used to perform the sequential reactions in alkaline and acid medium, followed by smartphone-based digital-image colorimetry.

2. Experimental

2.1. Reagents, solutions and materials

Solutions were prepared using analytical grade reagents dissolved in purified water (resistivity > 18 MΩ cm) obtained from Milli-RO 12 plus Milli-Q station (Millipore, Bedford, MA, USA).

Reagent solutions of 0.30 mol L^{-1} hydroxylamine or sodium hydroxide were prepared by dissolution of 1.15 g $NH_2OH.HCl$ or 0.600 g NaOH (both from Panreac) in 5 mL of water and making the final volume to 50 mL with ethanol (Merck). A 10 mmol L^{-1} Fe(III) solution was prepared by dissolution of 0.240 g of $NH_4Fe(SO_4)_2{\cdot}12H_2O$ (Panreac) in 20 mL of 1.60 mol L^{-1} HNO_3 (Panreac) and the volume was made up with water to 50 mL, obtaining a final concentration of 0.65 mol L^{-1} HNO_3.

Two kinds of diesel, either containing less than 10 ppm of sulfur (diesel S10, Petrobras, Brazil) or less than 500 ppm of sulfur (diesel S10, Petrobras, Brazil) were used to prepare blends with biodiesel produced from different feedstocks: 70% (v/v) soybean oil plus 30% (v/v) tallow (samples 1, 3 and 8); 90% (v/v) soybean oil plus 10% (v/v) tallow (samples 2 and 5); 90% (v/v) soybean oil plus 10% (v/v) cotton oil (sample 4); 100% (v/v) soybean oil (samples 6 and 7) and 93% (v/v) soybean oil, 5% (v/v) cotton oil, and 2% (v/v) tallow (sample 9).

Reference solutions within 0.1–0.6% (v/v) methyl linoleate were prepared by dilution of a 99% (v/v) stock solution (Sigma) in anhydrous ethanol. Diesel blends with different amounts of biodiesel were analyzed by MIR as reference technique [25].

The pNIPAM polymer was prepared as follows: 640 mg of N-isopropylacrylamide (Aldrich), 80 mg of dextran from *Leuconostoc ssp* (Fluka), and 16 mg of N,N-methylenebis-acrylamide (Sigma Aldrich) were dissolved in 4 mL of purified water and posteriorly 200 μL of a 65 mmol L^{-1} potassium persulfate (Panreac) solution and 48 μL of *N,N,N′, N′*-tetramethylethylenediamine solution (Sigma Aldrich) were added. The mixture was placed in a Bio-Rad mold with 0.75 mm spacers at 30 °C for 1 h to polymerize, achieving a 8 × 8 cm polymer, which was stored in a vessel with water [19]. For absorption of Fe(III) solution, the pNIPAM was cut manually into 4 × 5 mm pieces and dried at 40 ºC in a hot plate before immersion in the 10 mmol L^{-1} Fe(III)/ 0.65 mol L^{-1} HNO_3 solution for 30 min. The material was stored under refrigeration at 5 ºC until use.

Superabsorbent Flexicel (Evax Liberty/Super Alas, Procter & Gamble) and methacrylate sheet were used as reaction support for fabrication of the microfluidic device, respectively.

2.2. Apparatus

A laser printer (Rayjet 50 Laser Engraver, Austria) was used to engrave the plastic microfluidic device. A vortex (Boeco, Germany, model BOE 8062000) and ultrasound bath (Selecta, model 113834)

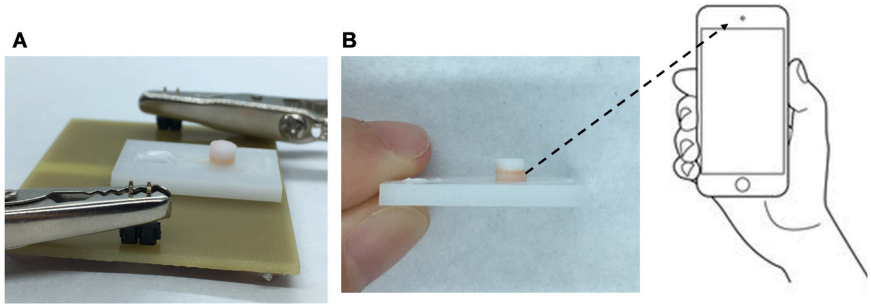

Fig. 2. Photography of the microfluidic device (A) and region for acquisition of digital images (B).

were used for reagents dissolution.

Reaction supports prepared from Flexicel superabsorbent were cut as disks with 4 mm diameter using a perforator (KNIPEX 90 70 220). pNIPAM of 0.75, 1.5, and 1.0 mm thicknesses were prepared using modules for Mini-PROTEAN Tetra electrophoresis system composed by tetra cell casting stand and clamps BIO-RAD (model 1658050), glass plates (model 1653312), short plates (model 1653308), and gaskets (model 1653305).

A portable commercial box for photography (24 ×23 x 22 cm; weight of 281 g) internally white, with 20 LED (*PULUZ*, China) at the bottom (height with 10 cm) was used to obtain the digital images with an iPhone (SE) (Apple, Foxconn, Jundiai, SP, Brazil), equipped with an 8 mega-pixels camera and lens aperture of f/2.2. All images were taken with camera flash and zoom disabled. RGB values were acquired with ImageJ® software (1.53 K, Wayne Rasband and Contributors, National Institutes of Health, USA) with a ROI of 60 × 130 pixels.

A resistive heater with a 22 Ω equivalent resistance composed by six 47 Ω surface mount device (SMD) resistors and a rated power of 3 W was fabricated on a printed circuit board (see Fig. S1). It was used to induce the pNIPAM phase transition by heating, by applying the appropriate electric voltage with an E3616A power supply (Keysight Tech. Santa Rosa, CA, USA). With this configuration, an area of 15 × 15 mm^2 with a stable and adjustable temperature was achieved. To determine the relationship between voltage and temperature, a previous calibration was made at different voltages obtaining an excellent linear trend: $T = 11.9 \cdot V - 2.63$ ($R^2 = 0.999$), where V is the voltage in volts and T is the temperature given in Celsius degrees.

2.3. Device fabrication

The microfluidic device was built up from a rectangular methacrylate sheet (2.7 ×1.7 cm) with 3 mm thickness (Fig. 1). A squared 25 mm^2

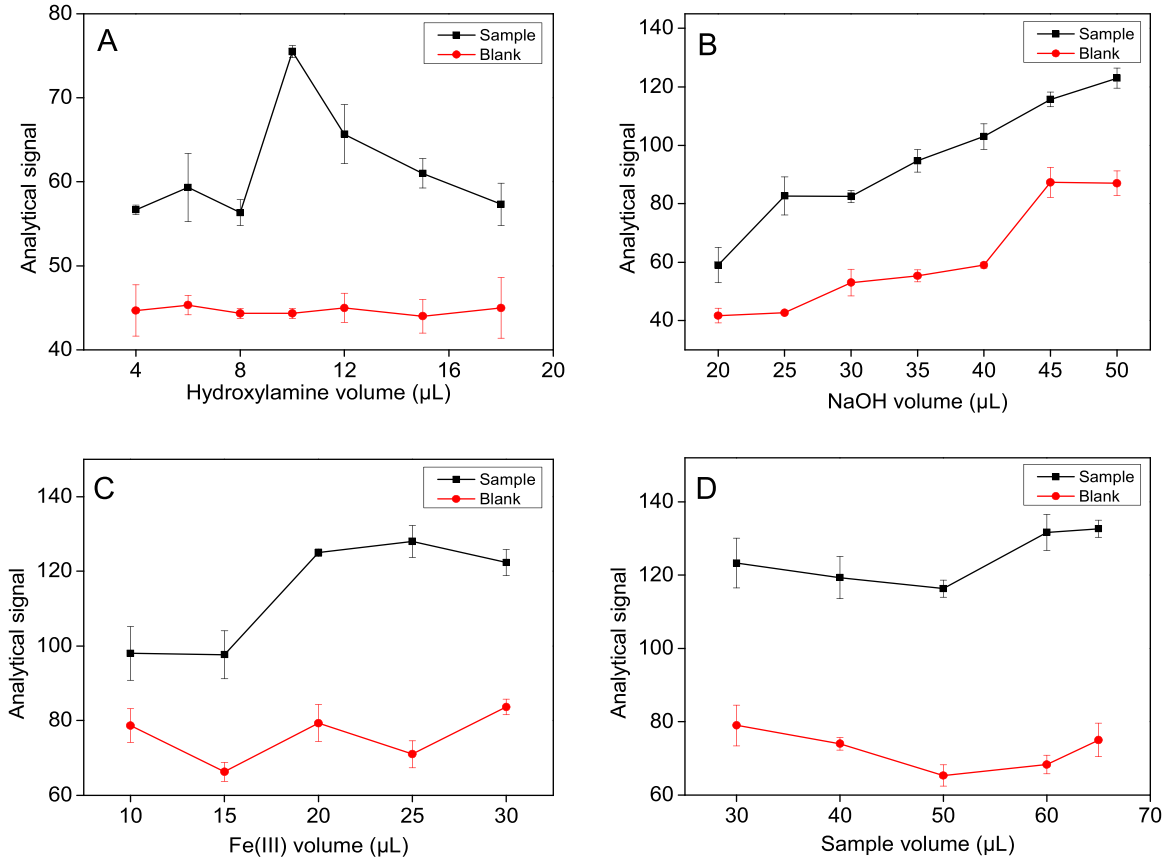

Fig. 3. Effect of volumes of (A) hydroxylamine, (B) NaOH, (C) Fe(III), and (D) sample solutions on the blank and analytical responses. Initial experimental conditions: 50 μL of 0.4%v/v methyl linoleate, 30 μL of 0.30 mol L^{-1} NaOH, 20 μL of 10 mmol L^{-1} Fe(III) in 0.65 mol L^{-1} HNO_3, and 15 min of reaction (hydroxamic acid formation). Results refer to mean values and estimates of standard deviations (n = 3).

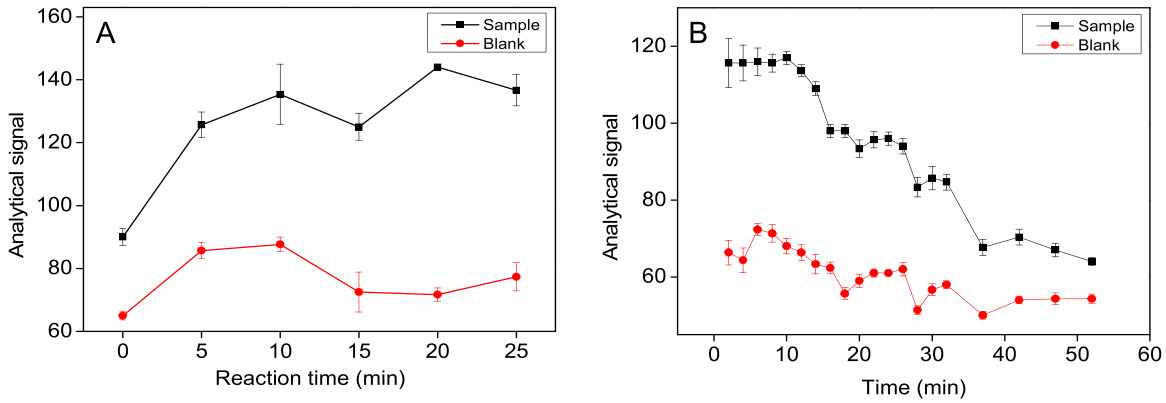

Fig. 4. Effect of (A) reaction time on hydroxamate formation and (B) stability of the Fe(III)-hydroxamate complex. Experimental conditions: 60 μL of 0.4%v/v methyl linoleate, 10 μL of 0.30 mol L^{-1} NH_2OH, 40 μL of 0.30 mol L^{-1} NaOH, 25 μL of 10 mmol L^{-1} Fe(III) in 0.65 mol L^{-1} HNO_3. Results refer to mean values and estimates of standard deviations. (n = 3).

Table 1
Recoveries of biodiesel from different raw materials added to different commercial diesel.

Raw material % (v/v)	Biodiesel % (v/v)*		Recovery (%)
	Added	Found	
Blends with diesel S10			
Soybean oil/animal fat (70/30)	7.5	8.1 ± 0.6	108 ± 8
Soybean oil/animal fat (90/10)	10.0	10.9 ± 0.3	111 ± 3
Soybean oil/animal fat (70/30)	10.0	9.8 ± 0.8	98 ± 8
Soybean/cotton oils (90/10)	15.0	16.3 ± 1.9	109 ± 13
Blends with diesel S500			
Soybean oil/animal fat (90/10)	7.5	8.6 ± 0.7	115 ± 10
Soybean oil (100)	10.0	10.0 ± 0.4	100 ± 4
Soybean oil (100)	15.0	15.5 ± 0.3	104 ± 2
Soybean oil/animal fat (70/30)	20.0	18.1 ± 0.3	90 ± 2
Soybean and cotton oils/animal fat (93/5/2)	25.0	22.2 ± 0.7	88 ± 3

* Mean ± standard deviation (n = 3)

reagent area (0.5 mm depth) and a circular sensing area (4.0 mm diameter and 1.0 mm depth) were engraved in the device to accommodate the pNIPAM piece and the cylindrical reaction support, respectively. These sections were connected by an 8-mm long channel (1.0 mm wide and 1.0 mm depth). The device was placed over the resistive heater, as indicated in Fig. 1.

2.4. Procedure

The analytical procedure was carried out by adding 60 μL of sample (diluted 1:50 v/v in anhydrous ethanol) in the reaction support (Flexicel cylinder) (Fig. 2). After 10 min, 10 μL of the 0.30 mol L^{-1} hydroxylamine hydrochloride and 40 μL of the 0.30 mol L^{-1} NaOH solutions were added directly on the support. After 20 min, the Fe(III) solution was released from the pNIPAM (Fig. 1a) by warming it at 42 °C after applying a voltage of 4.0 V to the heater (Supplementary Material, item 1). Colorimetric measurements were carried out by taking a lateral photograph of the reaction cylinder with a cell phone integrated camera, under controlled illumination, and further RGB values were extracted (Fig. 2B).

3. Results and discussion

3.1. General aspects

Hydroxamic acids are N-acyl derivatives of esters, usually produced from reaction with hydroxylamine in different polar solvents. Strong bases are needed to generate free hydroxylamine from hydroxylamine hydrochloride [26]. Hydroxamic acids contain a bidentate group able to form complexes via substitution of the hydrogen atom by a metal cation, such as Fe(III), V(V), and Cu(II), with ring closure via the carbonyl oxygen atom [9,27].

The sensing scheme used in this study consists of the hydroxamation reaction of alkyl esters from biodiesel with hydroxylamine in alkaline medium (Eq. (1)) followed by complexation with a metal, e.g. Fe(III), forming a colored complex (Eq. (2)). The latter reaction is carried out in acidic medium to avoid the hydrolysis of the metal ion.

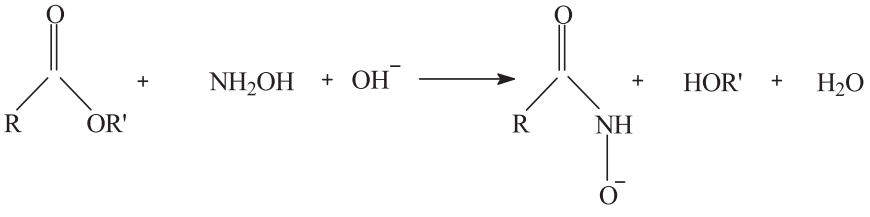

(1)

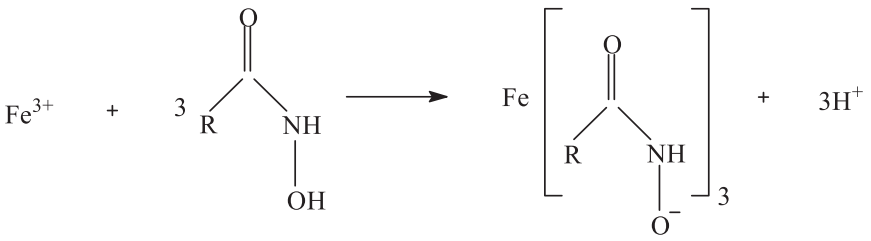

(2)

Different metallic ions were evaluated for sensing the hydroxamic acids (namely Fe(III), V(V) and Cu(II) in both HCl and HNO_3 media). Product formation was observed only with Fe(III) and V(V) in HNO_3, but only the Fe(III) complex was stable under working conditions. Therefore, Fe(III) in HNO_3 was selected for further experiments.

A microfluidic device was designed with the aim to simplify the analytical procedure for alkyl esters determination, including all the analytical operations involved in analyte derivatization. The device, engraved on a methacrylate sheet, consists of three parts: a) a reagent repository where a piece of pNIPAM is accommodated; b) a cylindrical section where a piece of the support for reaction and sensing is placed; c) an open sloped channel to connect the reagent repository to the reaction support.

The derivatization and recognition reactions were evaluated on different supports such as paper, cellulose acetate, fiberglass, cloths (cotton sarge, flannel, and 100% polyester), and the super adsorbent Flexicel superabsorbent, with only the latter yielding satisfactory and reproducible results. The lack of reproducibility observed in other materials was probably related to the non-uniform distribution of the reaction product, because of the uncontrolled evaporation of ethanol used to prepare reagents as well as for sample dilution. This solvent is needed to ensure the interaction between the hydrophobic analyte and the hydrophilic reagents (See experimental details in the Supplementary Material).

The recognition reaction originates a colored complex on Flexicel cylinder that is measured by digital-image colorimetry. Analytical signals were obtained as the reflected radiation intensity from the green channel (G) of the RGB color system, which is complementary to the absorption product. The G values were subtracted from full scale vale (255) to yield analytical responses proportional to the color intensities.

3.2. Procedure optimization

Methyl linoleate is the main ester produced by transesterification of soybean oil, which is the main raw material for biodiesel production [9]. Hence, it was selected as the model species for procedure optimization and calibration.

The procedure was optimized by the univariate method to maximize the analytical response and to reduce reagents consumption. Analyte derivatization and measurements were carried out directly on the reaction support. Based on a previous study [20], reagent concentrations were initially fixed at 0.30 mol L^{-1} hydroxylamine hydrochloride, 0.30 mol L^{-1} NaOH, and 10 mmol L^{-1} Fe(III) in 0.65 mol L^{-1} HNO_3, whereas the effect of sample and reagent volumes, as well as reaction times, were evaluated (Fig. 3). The experiments were performed on the Flexicel cylinder described in item 2.1. Moreover, the pNIPAM was evaluated as a repository for both NH_2OH and Fe(III) solutions.

A hydroxylamine volume of 10 μL was selected as optimal because it leaded to the highest difference from the analytical response and the blank value (Fig. 3A). While lower volumes hindered the analytical response due to the lack of reagent, higher amounts favored the reduction of Fe(III) to Fe(II), thus lessening the formation of the metal complex. This reagent concentration ensures a 3-fold reagent excess in relation to the higher methyl linoleate concentration assayed (0.6%v/v). When a single solution containing hydroxylamine and NaOH was evaluated as reagent, the slope of the analytical curve decreased ca. 30%. Because of this aspect and the lower stability of hydroxylamine in an alkaline medium [9], reagents prepared separately were preferred.

As shown in Fig. 3B, both analytical and blank signals increased linearly with the volume of NaOH. A high NaOH concentration favors formation of hydroxamate but also causes precipitation of $Fe(OH)_3$. The latter process increases blank values by a combination of light scattering and radiation absorption (brown suspension) and reduces the amount of the free metal ion, thus hindering the formation of the Fe(III)-hydroxamate complex. As these effects were more severe from 45 μL volumes, 40 μL was selected for subsequent experiments, in order to maximize the difference of the analytical response from the blank.

The volume of the acidic Fe(III) solution needs to ensure excess of metal ion to form the hydroxamate complex (1:3 metal/ligand stoichiometry, Eq. 2) and acid to neutralize the excess of NaOH from the previous derivatization reaction to avoid $Fe(OH)_3$ precipitation. These conditions were reached with a 25 μL of reagent, which resulted in the highest difference from the analytical response and blank value (Fig. 3C). A slight decrease in the analytical signal was observed for higher reagent volumes because the excess of acid hinders the complex formation, as hydroxamate ligand is the conjugate base of a weak hydroxamic acid. Regarding the sample volume, the highest response was observed with 60 μL (Fig. 3D).

Under the optimized sample and reagent volumes, the effect of the reaction time on formation of hydroxamate was evaluated. Previous results indicated that this reaction is relatively slow, demanding 15 min to achieve the steady state at ambient temperature [9]. As shown in Fig. 4A, the analytical signal increased until 20 min of reaction, which was the selected time for further work. Aiming at colorimetric measurements, it is desirable the formation of a stable complex on the support. As shown in Fig. 4B, the formed complex is stable for a period of 10 min, which suffices to capture the images from the support.

The pNIPAM was evaluated as a repository for reagents (hydroxylamine in NaOH and Fe(III) in HNO_3). It was found that the polymer efficiently retained and released the acidic Fe(III) solution, however it was not capable of retaining hydroxylamine in basic medium. Therefore, pNIPAM was evaluated as repository of Fe(III) solution in HNO_3 by mass difference in pNIPAM polymer of three different thicknesses (0.75, 1.0 or 1.5 mm) and different sizes (2 ×2, 2 ×3, 3 ×3, 3 ×4, 4 ×4, and 4 ×5 mm^2) to find the best condition to absorb 25 μL Fe(III) solution in HNO_3, that was previously defined as the optimal volume (Fig. 3C). Solution absorption increased with both polymer size and thicknesses (Supplementary Material, Fig. S2) and absorption of 25 μL was achieved using a (4 ×5) mm^2 piece of polymer with 1.5 mm thickness. Thus, the reagent compartment of the microfluidic device was set at (5 ×5) mm^2 and 1.5 mm depth. The connecting channel was set at 0.5 mm, which was the minimum width to allow the solution to flow from the pNIPAM to the reaction support. The length was set to 8 mm in order to avoid the heating of the reaction support during the release of Fe(III) solution from pNIPAM. Dimensions of the reaction support were kept at 4 mm diameter and 3 mm depth, which were suitable to carry out the chemical

Table 2
Biodiesel contents in diesel blends determined by the proposed and reference procedures [25].

Sample	Biodiesel % (v/v)*		
	Proposed	Reference	* *F_{cal}
1	13.4 ± 1.5	14.8 ± 0.5	9.0
2	12.7 ± 0.4	14.1 ± 0.2	4.0
3	16.4 ± 1.5	16.1 ± 0.7	4.6
4	15.7 ± 1.5	16.6 ± 0.7	4.6
5	22.1 ± 2.9	19.2 ± 1.0	8.4
6	19.5 ± 0.1	18.6 ± 0.2	4.0

* Mean ± standard deviation (n = 3); * *$F_{critical}$ = 19 (95% confidence level)

reactions and a reliable image acquisition.

After optimization, the order of addition of the reagents to the reaction support was evaluated. Product formation was not observed when hydroxylamine and NaOH were added before the sample solution, due to the poor interaction with the sample. It was observed that the denser hydroalcoholic reagent flows to the bottom of the support, whereas the sample solution tended to stay on the top.

3.3. Analytical features and application

Under optimized conditions, a linear response was obtained in the range 0.1–0.6%(v/v) methyl linoleate, described by the equation Analytical signal = 69.6 + 2.1 C (r = 0.999), as show in Supplementary Material, Fig. S3. This range corresponds to 5–30% (v/v) of biodiesel in the diesel blend. The coefficient of variation was estimated at 4.0% (n = 10) and the detection limit was estimated at 0.04% (v/v), as the lowest methyl linoleate concentration that yielded an analytical response significantly different from the blank at the 95% confidence level. Each determination consumed 1.2 μL of sample, 230 μg hydroxylamine, 480 μg NaOH, 23 μg Fe(III), and equivalent to 1.2 μL of 69%(v/v) HNO_3. These amounts were up to 5-fold lower than those previously reported [9].

Recoveries within 88% and 115% were estimated for samples prepared from biodiesel obtained from different feedstocks mixed with different kinds of commercial diesel (Table 1). This demonstrates the absence of matrix effects and proves the feasibility of using external standard calibration, which is an important characteristic because different feedstocks are usual in industrial biodiesel production [2]. For accuracy assessment, the biodiesel amounts determined by the proposed and MIR [25] methods (Table 2) were compared. The paired t-test indicated that the results agreed at the 95% confidence level.

The precision of the proposed procedure was similar to Vis [6] and UV [28] spectrophotometric procedures and significantly better than using HPLC-UV [29]. With the applied 50-fold sample dilution, the limit of detection and the linear working range of the proposed procedure are in accordance with the minimum limit of biodiesel (e.g. 10%v/v in Brazil). The proposed procedure meets the green analytical chemistry requirements [30,31], as it consumes a less toxic solvent (ethanol instead of hexane [29] or heptane [6,28]) as well as microgram amounts of reagents. Moreover, solvent consumption is ca. 20 and 10-fold lower than the required in a flow-based procedure based on the lab-in-syringe approach [8] and spot test with digital-image photometry [9], respectively Supplementary Material, Table S1. Moreover, data acquisition by smartphone-based digital-image photometry makes the procedure more practical and portable, thus more attractive for POC.

4. Conclusions

A practical, green, and cost-effective microfluidic device was proposed for determining biodiesel in diesel blends using detection by digital images acquired with a smartphone camera. The analytical features such as linear response range, limits of detection and quantification, precision, and accuracy indicate that the proposed procedure is a reliable alternative for determining biodiesel in diesel blends. Using ethanol as a mediator solvent to dissolve both the sample and reagent minimized the risk of matrix effects from biodiesel produced from different feedstocks (soybean and cotton oils and animal fat) and made it feasible external standard calibration with ethanolic reference solutions. Even samples containing colored additives (yellow and red colorants for diesel S10 and S500, respectively) may be analyzed without effects of sample background absorption. The microfluidic device combined with image-processing proved to be an efficient platform for quantitative analysis aiming at fraud prevention.

CRediT authorship contribution statement

Samara Soares: Investigation, Validation, Formal analysis, Writing – original draft. **Celia E. Ramos-Lorente:** Investigation, Validation, Formal analysis, Writing – original draft. **Isidoro Ruiz-García:** Investigation, Validation. **Fabio R.P. Rocha:** Conceptualization, Validation, Formal analysis, Writing – original draft, Writing – review & editing, Supervision, Funding acquisition. **Miguel M. Erenas:** Conceptualization, Validation, Formal analysis, Writing – original draft, Writing – review & editing, Supervision. **Ignacio de Orbe-Payá:** Validation, Supervision, Methodology, Formal analysis. **Nuria Lopez-Ruiz:** Validation, Supervision, Methodology, Formal analysis. **Luis F. Capitán-Vallvey:** Validation, Writing – original draft, Resources, Writing – review & editing, Project administration, Funding acquisition.

Declaration of Competing Interest

The authors declare that they have no known competing financial interests or personal relationships that could have appeared to influence the work reported in this paper.

Data availability

Data will be made available on request.

Acknowledgments

The authors gratefully acknowledge the financial support from Fundação de Amparo à Pesquisa do Estado de São Paulo FAPESP (proc. 2021/12242–5 and 2018/07687–5). and the support from the Spanish "Ministerio de Economía y Competitividad" (Project PID2019–103938RB-I00) and Junta de Andalucía (Projects B-FQM-243-UGR18 and P18-RT-2961).

Appendix A. Supporting information

Supplementary data associated with this article can be found in the online version at doi:10.1016/j.snb.2023.134033.

References

[1] Z. Navas-Anguita, D. García-Gusano, D. Iribarren, A review of techno-economic data for road transportation fuels, Renew. Sustain. Energy Rev. 112 (2019) 11–26, https://doi.org/10.1016/j.rser.2019.05.041.
[2] G. Knothe, Analyzing biodiesel: Standards and other methods, J. Am. Oil Chem. Soc. 83 (2006) 823–833, https://doi.org/10.1007/s11746-006-5033-y.
[3] Introdução do biodiesel na matriz energética brasileira - Lei No 11.097, n.d. http://www.planalto.gov.br/ccivil_03/_ato2004–2006/2005/lei/l11097.htm.
[4] P. Bórawski, A. Bełdycka-Bórawska, E.J. Szymańska, K.J. Jankowski, B. Dubis, J. W. Dunn, Development of renewable energy sources market and biofuels in the European Union, J. Clean. Prod. 228 (2019) 467–484, https://doi.org/10.1016/j.jclepro.2019.04.242.
[5] G. Knothe, J.V. Gerpen, J. Krahl, The biodiesel handbook, 2nd ed., AOCS Publishing, Champaign, 2005. https://doi.org/10.1201/9781439822357.
[6] M.A.A. Silva, R.A. Correa, M.G.O. Tavares, N.R.Antoniosi Filho, A new spectrophotometric method for determination of biodiesel content in biodiesel/diesel blends, Fuel 143 (2015) 16–20, https://doi.org/10.1016/j.fuel.2014.10.048.

[7] R.P.M. Costa, T.C. Khalila, A.P.F. Santos, D.F. Andrade, L.A. D'Avila, Determination of biodiesel content in diesel using the colorimetric assay for hydroxamic acid, Quim. Nova 38 (2015) 563–569, https://doi.org/10.5935/0100-4042.20150039.
[8] S. Soares, W.R. Melchert, F.R.P. Rocha, A flow-based procedure exploiting the lab-in-syringe approach for the determination of ester content in biodiesel and diesel/biodiesel blends, Talanta 174 (2017) 556–561, https://doi.org/10.1016/j.talanta.2017.06.053.
[9] S. Soares, L.C. Nunes, W.R. Melchert, F.R.P. Rocha, Spot test exploiting smartphone-based digital images for determination of biodiesel in diesel blends, Microchem. J. 152 (2020), 104273, https://doi.org/10.1016/j.microc.2019.104273.
[10] R. Zeng, M. Qiu, Q. Wan, Z. Huang, X. Liu, D. Tang, D. Knopp, Smartphone-based electrochemical immunoassay for point-of-care detection of SARS-CoV-2 nucleocapsid protein, Anal. Chem. 94 (2022) 15155–15161, https://doi.org/10.1021/acs.analchem.2c03606.
[11] Y. Yang, E. Noviana, M.P. Nguyen, B.J. Geiss, D.S. Dandy, C.S. Henry, Paper-based microfluidic devices: emerging themes and applications, Anal. Chem. 89 (2017) 71–91, https://doi.org/10.1021/acs.analchem.6b04581.
[12] N. Convery, N. Gadegaard, 30 years of microfluidics, Micro Nano Eng. 2 (2019) 76–91, https://doi.org/10.1016/j.mne.2019.01.003.
[13] A.-G. Niculescu, C. Chircov, A.C. Bîrcă, A.M. Grumezescu, Fabrication and applications of microfluidic devices: a review, Int. J. Mol. Sci. 22 (2021) 1–26, https://doi.org/10.3390/ijms22042011.
[14] E. Noviana, T. Ozer, C.S. Carrell, J.S. Link, C. McMahon, I. Jang, C.S. Henry, Microfluidic paper-based analytical devices: from design to applications, Chem. Rev. 121 (2021) 11835–11885, https://doi.org/10.1021/acs.chemrev.0c01335.
[15] S. Sachdeva, R.W. Davis, A.K. Saha, Microfluidic point-of-care testing: commercial landscape and future directions, Front. Bioeng. Biotechnol. 8 (2021), 602659, https://doi.org/10.3389/fbioe.2020.602659.
[16] M.D. Fernández-Ramos, A.L. Ogunneye, N.A.A. Babarinde, M.M. Erenas, L. F. Capitán-Vallvey, Bioactive microfluidic paper device for pesticide determination in waters, Talanta 218 (2020), 121108, https://doi.org/10.1016/j.talanta.2020.121108.
[17] Y. Lin, Q. Zhou, J. Li, J. Shu, Z. Qiu, Y. Lin, D. Tang, Magnetic graphene nanosheet-based microfluidic device for homogeneous real-time electronic monitoring of pyrophosphatase activity using enzymatic hydrolysate-induced release of copper ion, Anal. Chem. 88 (2016) 1030–1038, https://doi.org/10.1021/acs.analchem.5b04005.
[18] M.M. Erenas, B. Carrillo-Aguilera, K. Cantrell, S. Gonzalez-Chocano, I.M. Perez Vargas-Sansalvador, I. Orbe-Payá, L.F. Capitan-Vallvey, Real time monitoring of glucose in whole blood by smartphone, Biosens. Bioelectron. 136 (2019) 47–52, https://doi.org/10.1016/j.bios.2019.04.024.
[19] M. Oliveira Krambeck Franco, W.T. Suarez, V.B. Santos, I.S. Resque, M.H. Santos, L.F. Capitán-Vallvey, Microanalysis based on paper device functionalized with cuprizone to determine Cu2+ in sugar cane spirits using a smartphone, Spectrochim. Acta Part A Mol. Biomol. Spectrosc. 253 (2021), 119580, https://doi.org/10.1016/j.saa.2021.119580.
[20] W. Luo, J. Deng, J. He, Z. Han, C. Huang, Y. Li, Q. Fu, H. Chen, A smartphone-based multi-wavelength photometer for on-site detection of the liquid colorimetric assays for clinical biochemical analyses, Sens. Actuators B Chem. 329 (2021), 129266, https://doi.org/10.1016/j.snb.2020.129266.
[21] M.S.M.S.F. Acevedo, M.J.A. Lima, C.F. Nascimento, F.R.P. Rocha, A green and cost-effective procedure for determination of anionic surfactants in milk with liquid-liquid microextraction and smartphone-based photometric detection, Microchem. J. 143 (2018) 259–263, https://doi.org/10.1016/j.microc.2018.08.002.
[22] S.K. Schlesner, M. Voss, G.A. Helfer, A.B. Costa, A.J. Cichoski, R. Wagner, J. S. Barin, Smartphone-based miniaturized, green and rapid methods for the colorimetric determination of sugar in soft drinks, Green. Anal. Chem. 1 (2022), 100003, https://doi.org/10.1016/j.greeac.2022.100003.
[23] E. Trofimchuk, A. Nilghaz, S. Sun, X. Lu, Determination of norfloxacin residues in foods by exploiting the coffee-ring effect and paper-based microfluidics device coupling with smartphone-based detection, J. Food Sci. 85 (2020) 736–743, https://doi.org/10.1111/1750-3841.15039.
[24] M. Ariza-Avidad, M. Agudo-Acemel, A. Salinas-Castillo, L.F. Capitán-Vallvey, Inkjet-printed disposable metal complexing indicator-displacement assay for sulphide determination in water, Anal. Chim. Acta 872 (2015) 55–62, https://doi.org/10.1016/j.aca.2015.02.045.
[25] European Standard – EN 14078, Liquid petroleum products – Determination of fatty methyl ester (FAME) content in middle distillates – Infrared spectrometry method, 2014.
[26] M.A. Alam, Methods for hydroxamic acid synthesis, Curr. Org. Chem. 23 (2019) 978–993, https://doi.org/10.2174/1385272823666190424142821.
[27] Y.K. Agrawal, Hydroxamic acids and their metal complexes, Russ. Chem. Rev. 48 (1979) 948–963, https://doi.org/10.1070/rc1979v048n10abeh002422.
[28] A. Zawadzki, D.S. Shrestha, B. He, Biodiesel blend level detection using ultraviolet absorption spectra, Trans. ASABE 50 (2007) 1349–1353.
[29] T.A. Foglia, K.C. Jones, J.G. Phillips, Determination of biodiesel and triacylglycerols in diesel fuel by LC, Chromatographia 62 (2005) 115–119, https://doi.org/10.1365/s10337-005-0599-3.
[30] R. Rosa, M. Pini, G.M. Cappucci, A.M. Ferrari, Principles and indicators for assessing the environmental dimension of sustainability within green and sustainable chemistry, Curr. Opin. Green. Sustain. Chem. 37 (2022), 100654, https://doi.org/10.1016/j.cogsc.2022.100654.
[31] R.S. Amais, L.S.G. Teixeira, F.R.P. Rocha, Greener procedures for biodiesel quality control, Anal. Methods 7 (2015) 4396–4418, https://doi.org/10.1039/c5ay00530b.

Samara Soares is graduate in Biofuel Technology and doctorate student in Sciences at Center for Nuclear Energy in Agriculture, University of Sao Paulo. She is expert in Biofuels production and analysis, Spectroanalysis, Sample preparation, and Green analytical chemistry. She has worked in the development of innovative analytical approaches for biodiesel analysis, mainly exploiting flow analysis, spot tests, digital-image photometry, and novel calibration approaches.

Celia E. Ramos-Lorente received her degree in chemistry at the University of Granada in 2019. She is currently finishing a combination of two master's programs in Teaching Training in Obligatory Secondary and Upper Secondary School Education, Vocational Training and Languages and in Chemical Sciences and Technologies at the Official Post-graduate School in the same university. She is interested in colorimetric microfluidic thread and cloth-based sensors.

Isidoro Ruiz-García was born in Granada, Spain, in 1996. He received the B.S. degree in telecommunications engineering, and the M.Sc. degree in electronic engineering from the University of Granada, Granada, Spain, in 2018 and 2019. Since 2021, he is a PhD student of information and communication technologies in the University of Granada.Currently he works as predoctoral research fellow in the ECSens group (Electronic and Chemical sensing solutions) at University of Granada. His research interests include real-time flow monitoring in capillary microfluidic devices, sensing systems for health and sport, and the effects of irradiation in optoelectronic devices.

Fábio R. P. Rocha is graduate in Chemistry and PhD in Sciences. He is expert in Flow analysis, Spectroanalysis, Sample preparation, and Green analytical chemistry. He works at the Center for Nuclear Energy in Agriculture, University of Sao Paulo and is researcher of National Council for Scientific and Technological Development, Brazil. He authored 161 articles (3524 citations, h = 32), 2 books, and 7 book chapters, and concluded 32 academic supervisions.

Miguel M. Erenas received the MSc degree (2004) and the PhD degree in Analytical Chemistry (2011) from the University of Granada (Granada, Spain). He is Assistant Professor at the Department of Analytical Chemistry, University of Granada. His research interests include the use of imaging along with microfluidic disposable sensors based on thread and paper for bioanalysis and food quality analysis.

Ignacio de Orbe-Payá is Associate Professor of the Department of Analytical Chemistry at the University of Granada (Spain). His main areas of research are the development of the sensing phases for their use as chemical sensors in the determination of inorganic ions in several matrices; multivariate calibration methods for the quality control of pharmaceutical products and development of analytical methodology using solid-phase spectrometry.

Nuria López-Ruiz was born in Barcelona, Spain, in 1985. She received the B.S. degree in telecommunications engineering, the B.S. degree in electronic engineering, the M.Sc. degree in telecommunications engineering, and the Ph.D. degree in information and communication technologies from the University of Granada, Granada, Spain, in 2008, 2009, 2010, and 2014, respectively. She is currently an Associate Professor with the University of Granada, Spain. Her current research interests include the study of different optical sensors for environmental and biological measurements, the development of paper-based microfluidic platforms, and the design of portable electronic instrumentation and smartphone applications associated with them.

Luis F. Capitan-Vallvey, Full Professor of Analytical Chemistry at the University of Granada, received his BSc in Chemistry (1973) and PhD in Chemistry (1986) from the Faculty of Sciences, University of Granada (Spain). In 1983, he founded the Solid Phase Spectrometry group (GSB) and in 2000, together with Prof. Palma López, the interdisciplinary group ECsens, which includes Chemists, Physicists and Electrical and Computer Engineers at the University of Granada. His current research interests are the design, development and fabrication of sensors and portable instrumentation for environmental, health and food analysis and monitoring. Recently is interested in printing chemical sensor and capillary-based microfluidic devices.